Theor Chim Acta (1994) 87: 321–333

Theoretica Chimica Acta

On the dimerization process of nitroso compounds.

A theoretical study of the reaction 2 HNO → $(HNO)_2$

W. Lüttke[1], P. N. Skancke[2], M. Traetteberg[3]

[1] Organisch-Chemisches Institut der Universität Göttingen, Tammannstrasse 2, D-37077 Göttingen, Germany

[2] Department of Chemistry, The University of Tromsø, N-9037 Tromsø, Norway

[3] Department of Chemistry, University of Trondheim, AVH, N-7055 Dragvoll, Norway

Received December 21, 1992/Accepted April 26 1993

Summary. Many organic C-nitroso compounds R–NO form stable dimers with a covalent NN bond. To gain insight into the dimerization reaction 2 R–NO⇄ $(R–NO)_2$ a theoretical study of the dimerization to a *trans*-form was performed using HNO as a model compound. Complete geometry optimizations were carried out at the HF, MP2 and QCISD levels using a 6-31G* basis. In the stationary points energies were calculated at the MP4(SDTQ) and QCISD(T) levels. For the equilibrium structure of the monomer and dimers stable RHF solutions were found, whereas for the TS UHF and UMPn calculations were applied. Extensive spin contamination was found in the UHF wavefunction, and projections up to $s + 4$ were invoked. Relative energies were corrected for differences in ZPE. Calculations were made (a) for the least-motion path (C_{2h} symmetry) and (b) for a path with complete relaxation of all internal coordinates. Along the latter path a TS having virtually C_i symmetry was found. Along path (a) an activation energy of around 150 kcal/mol was predicted, in conformity with a symmetry forbidden reaction. On the relaxed path (b) the barrier to dimerization was estimated to be 10.7 kcal/mol at the MP4(SDTQ)//MP2 level, and 10.9 kcal/mol at the QCISD(T)//QCISD level. Unscaled ZPE corrections, calculated at the SCF level, changed these values to 12.7 and 12.9 kcal/mol, respectively. The reaction energy for the dimerization process is predicted to be − 17.2 kcal/mol at the MP4(SDTQ)//MP2 level corrected for ZPE. Calculations at the G1 level gave a corresponding value of − 16.4 kcal/mol. The equilibrium constant for the association to the *trans* dimer is estimated to be $K_p = 259$ atm, indicating that the dimer should be an observable species in the gas phase.

Key words: Nitroso compounds – Dimerization – Transition state – Quantum chemistry – *Ab initio*

Correspondence to: P. N. Skancke

1 Introduction

Solutions of many organic nitroso compounds (R–NO) in organic solvents, where the NO group is bonded to a carbon atom (C-nitroso compounds), display blue or bluegreen colours, due to a weak absorption band in the visible region ($\lambda \sim 700$ nm, $\varepsilon < 50$) [1]. In the crystalline state, however, most of these compounds are colourless or at most pale yellow. The colour intensity of a solution of a C-nitroso compound depends on the nature of the organic group (R) and decreases with decreasing temperature and with increasing concentration.

The reason for these phenomena was elucidated by Piloty [2] already in 1898, based on cryoscopic molecular weight measurements: faintly coloured (R–NO)-solutions contain a significant proportion of dimeric molecules in equilibrium with monomers:

$$\underset{1}{2\,\text{R–NO}} \rightleftarrows \underset{2}{(\text{R–NO})_2} \tag{1}$$

Piloty therefore concluded that the colourless crystals of C-nitroso compounds were exclusively built from dimeric units. His assumption was verified in 1950 by two X-ray structure determinations [3, 4], and in 1956 by vibrational spectroscopy [5–9]. The X-ray studies showed that in the dimers the nitrogen atoms of the two R–NO subunits were bonded directly together (species 3), as first suggested by Hammick [10]. The observed NN distance of 1.31 Å indicates a certain degree of double bond character, when compared to the NN distance in hydrazine (1.447 Å) and in azomethane (1.247 Å), respectively. See Table 2. The dimers may therefore be characterized as azo-dioxy compounds or – more correctly – as diazene-1,2-dioxides. Such compounds should in principle exist in two stereoisomeric forms. In accordance with this Gowenlock, Trotman and Chilton [11, 12] succeeded in 1953 to prepare the *trans* (species 3) as well as the *cis* (species 4) isomer of bis-nitrosomethane. The configurations of these stereoisomers were later confirmed by X-ray structure determinations [13, 14] and by quantum mechanical calculations [15].

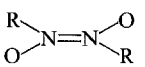

3

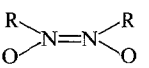

4

(2)

In accordance with the theoretical arguments of Orgel [16] and of Wu et al. [17], and the spectroscopic observations by Herzberg [18], the electron distribution in an R–NO monomer corresponds to that of a closed-shell singlet molecular ground state. An R–NO molecule is therefore expected to be relatively stable, and it is accordingly not obvious that R–NO monomers will dimerize spontaneously.

A comparison between the electron configuration in the monomers and in the dimers suggests that the dimerization process requires a reorganization of the electron distribution in the R–NO subunits [7, 19, 20]. An experimental evidence, indicating that this indeed happens, is the observed colour difference between monomers and dimers. The blue to green colour of monomer solutions [1] is due to a weak long wavelength absorption band caused by an $n \rightarrow \pi^*$ transition involving the electron lone-pair that is predominantly localized on the nitrogen atom [7, 16, 19–24]. This $n \rightarrow \pi^*$ absorption band disappears when the nitrogen lone-pair in

the monomer is used to form the NN bond in the dimer or, analogously, when a nitroso monomer is oxidized to a nitroso compound (species 6) [25].

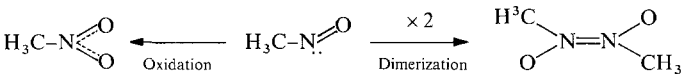

6 1 3

UV/Vis. Spectroscopic data:

π_{max}:	280 nm [26]	665 nm [1]	286 nm [11]
ε_{max}:	16	20	10200

HMO π bond orders:

p(NO):	0.707	0.989	0.454
p(NN):	–	–	0.711

Considering that a nitroso monomer, R–N=O, has two π electrons, while the dimer, $(R–NO)_2$, accomodates six such electrons, it is obvious that during the dimerization process the two nitrogen lone-pairs in the monomers are converted to an NN σ-bond and to an occupancy in the π-electron system of the dimer, as characterized by an intensive UV absorption band (cfr. species 3 above) due to a $\pi \rightarrow \pi^*$ transition.

These differences in π-electron distribution in the RNO units in the monomer and in the dimer are also reflected by the changes in HMO π bond orders (see above). The HMO π bond orders are closely related to the experimentally obtained NO and NN bond lengths (see Table 2 and Fig. 1), as well as to the NO and NN bond stretching frequencies of the monomers and dimers, respectively [7–9, 19]. These observations give additional support to the view that an extensive reorganization of electrons takes place during the dimerization process.

Hoffmann, Gleiter and Mallory have studied the dimerization of HNO on the basis of EHT calculations [27], and their work is therefore relevant to the structural implications of R–NO monomer and dimers pointed at above. They found that the energy barrier of the dimerization process is primarily determined by the energy involved in the reorganization of the electrons. The path of the approach of the two monomers is therefore crucial for the magnitude of the energy barrier. The monomers can not react in a least-motion path since this would result in an orbital symmetry forbidden reaction. Instead a nonplanar non-least-motion path, where the nitrogen lone pair of one monomer impinges on the π system of the other, turned out to be energetically far more favourable.

Yamabe et al. [28] have made a theoretical study of the dimerization of nitrosomethane, and of the related *cis/trans* isomerization of azodioxymethane. With the aid of state correlation diagrams [29] they systematically studied alternative reaction paths. For the dimerization process leading to the *trans* form they obtained a reaction path retaining C_i symmetry, which is symmetry-allowed on the ground state surface, in agreement with that proposed by Hoffman, Gleiter and Mallory [27].

The dimerization reaction of nitroso compounds has been properly accounted for as far as symmetry constraints on the reaction path are concerned. The question

of how the geometry and energy of the reacting system vary quantitatively during the reaction remained, however, unanswered. The same applies to the nature of the transition state for the process. Because of the reorganization of the electrons that takes place during the reaction an adequate description of the electron distribution – at least in the region close to the transition state-requires unrestricted calculations. A reliable estimate of the energetics of the process will require an inclusion of electron correlation.

Heiberg [30] calculated the potential curves for the least-motion dissociation of *trans* dimeric nitroso-methane in its lowest singlet and triplet states using a limited CI approach. The open-shell configuration describing the disssociation into two triplet monomers was shown to have a significant influence on the singlet-state potential curve. Heiberg predicted an activation energy E_a of 39.7 kcal/mol for the dimerization of CH_3–NO and a dissociation energy ΔH of the dimer of 28.0 kcal/mol, compared to an experimental value of 16.6 kcal/mol [31]. It was pointed out that more extensive CI calculations were required in order to obtain a more accurate estimate of the dissociation energy.

In this paper we present results obtained from a theoretical study of the equilibrium reaction between monomer (**1**) and dimer forms (**3** and **4**) of HNO. We have studied the variation in geometry and energy along two different reaction paths: (a) the least-motion path and (b) a path resulting from a complete relaxation of all internal coordinates of the reacting system.

For computational reasons we have chosen two HNO monomers as a model for the dimerization of C-nitroso compounds. This requires an explanation, as the dimer of HNO has so far not been identified. A tautomer of the HNO dimer, HO–N=N–OH is, however, known [32], although it is not very stable. This compound, hyponitrous acid, may be formed from the monomers by an alternative reaction path, or it may be formed by a spontaneous rearrangement of initially formed dimer $(HNO)_2$. Another reason why the dimeric nitroxyl is not observed might be due to the competing or consecutive reaction $2\,HNO \rightarrow N_2O + 2\,H_2O$, the mechanism of which is not yet fully understood [33, 34]. The various competing reactions involving HNO monomers will probably take place in different regions on a continuous potential surface for thermal reactions.

A further indication supporting the assumption that the dimerization of H–NO and CH_3–NO will proceed by similar reaction paths is the fact that the results from experimental and theoretical structure studies show that the geometry, and also the vibrational and electronic spectra, of H–NO and CH_3–NO are very similar, see Table 2 and Refs. [1, 8]. For CH_3–NO, from which stable dimers are easily formed [11, 36, 37], the alternative reaction paths for H–NO discussed above are inaccessible. In this communication we will focus on the part of the surface describing the association of two HNO units to the *trans* form of the dimer.

2 Computational methods

For all the species included in this study we have used a 6-31G* basis set [38, 39]. The double-zeta functions should give sufficient flexibility to the description of the valence electrons, and the auxiliary polarization functions are supposed to give an adequate description of the polarity of the electron distribution. Geometry optimizations have been performed at the SCF, MP2 and the QCISD [40] levels where both spin restricted and spin unrestricted approaches have been applied. The

restricted SCF solutions were tested with respect to instability relative to unrestricted solutions. Energy differences have been estimated at higher levels of calculation. We have used CI calculations including all single and double exitations from a single determinant (CISD). Energies obtained in this way have been corrected for lack of size consistency. Alternatively we have used the Møller–Plesset perturbation approach up to fourth order, including single, double, triple and quadruple exitations (MP4(SDTQ)), and the QCISD(T) method. Where appropriate, energies have been corrected for spin contamination of the final wavefunctions. Corrections for differences in zero point vibrational energies (ZPE) calculated at the SCF, MP2 and QCISD levels have also been included. These energies are all unscaled. For the least-motion channel appropriate symmetry constraints have been invoked, whereas for the non-least-motion reaction no symmetry constraints have been introduced in the optimizations. Each stationary point on the potential surface has been characterized as a minimum or a col depending on whether it displays zero or one imaginary frequency, respectively.

In order to obtain a more accurate estimate of the reaction energy (ΔH) of the dimerization reaction, energy calculation of the dimer according to the G1 theory [41] was performed. The corresponding energy for monomer was taken from literature [41]. The program package Gaussian 90 [42] was used throughout the calculations.

3 Results and discussion

The electronic structures of the ground state and the low-lying states of the HNO monomer are known experimentally [43] and also from theoretical calculations [17, 44–50]. Our optimized structure parameters of the ground-state singlet (**10a**) obtained at different calculational levels are given in Table 1. They are in good agreement with the results of the experimental studies, see Table 2. The bond distances predicted at the SCF level are somewhat short as compared to the observed ones. Optimizations using correlated wavefunctions give a very good agreement with experiment. The lowest triplet state, $^3\mathbf{A}''$, species **10b**, reproduced in Fig. 1, has been optimized by the ROHF approximation. This state has a

Table 1. Geometry (in Å and degrees), energies (in a.u.) and zero-point energies (ZPE) (in kcal/mol) for HNO ground state obtained at different calculational levels. Basis 6-31G*

	HF	MP2	QCISD
R(N–O)	1.1752	1.2369	1.2218
R(N–H)	1.0317	1.0586	1.0641
∠(O–N–H)	108.79	107.37	107.93
E(a.u.)			
HF	− 129.78607		
MP2	− 130.11862	− 130.12459	
MP4(SDTQ)	− 130.14172	− 130.14806	
QCISD			− 130.13579
QCISD(T)			− 130.14677
ZPE (kcal/mol)	10.08	8.69	8.76

Table 2. Experimental molecular geometry data for RNO and related molecules. (Distances in Å, angles in degrees)

Molecule	R(N=O(N)) R(N–O(N))	R(N–R)	∠RNO ∠RNN	Ref.
H–N=O (r_0; θ_0)	1.212	1.063	108.6	[52]
H_3C–N=O (r_s; θ_s)	1.2112	1.4820	113.16	[a]
H_2N–OH (r_0; θ_0)	1.453	1.016 NH 0.962 OH	103.25 HNO 101.4 HON	[b]
H–N=N–H (r_0; θ_0)	1.252	1.028	106.85	[c]
H_3C–N=N–CH_3 (r_a; θ_a)	1.247	1.482	112.3	[d]
H_2N–NH_2 (r_{av}; θ_{av})	1.447	1.015	106; 112	[e]

[a] Turner PH, Cox AP (1978) J Chem Soc Faraday II 74:533
[b] Tsunekawa J (1972) J Phys Soc Japan 33:167
[c] Carlotti M, Johns JWC, Trombetti A (1974) Can J Phys 52:340
[d] Almenningen A, Anfinsen IM, Haaland A (1970) Acta Chem Scand 24:1230
[e] Kohata K, Fukuyama T, Kuchitsu K (1982) J Phys Chem 86:602

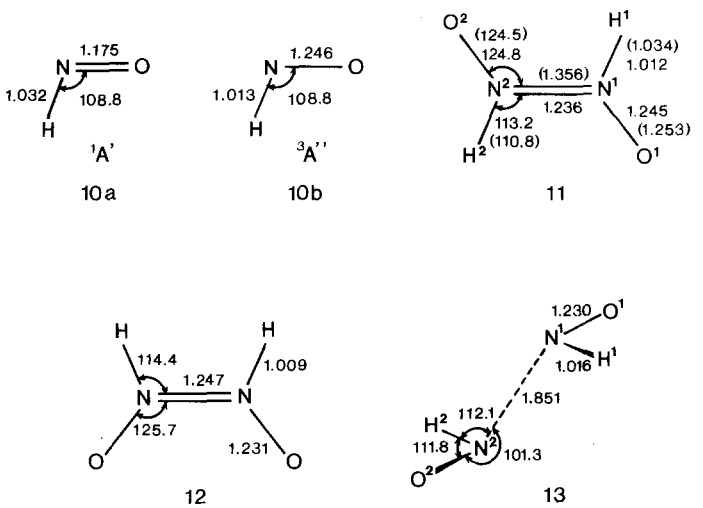

Fig. 1. Optimized geometry parameters for **10a** obtained by RHF and for **10b** obtained by ROHF. Basis 6-31G*. Parameters for **10a** obtained at higher levels of calculation are presented in Table 1. For the remaining species shown optimized geometry parameters are found in Tables 4 to 6

significant longer N–O bond than the ground state optimized at the RHF level, whereas the other structural parameters are virtually the same. For comparison both structures are given in Fig. 1. The singlet–triplet energy splitting, given in Table 3, is found to be 20.5 kcal/mol at the calculational level MP4(SDTQ)//SCF. The CI estimate gives a value of 16.0 kcal/mol. These values are significantly higher than the one obtained at the SCF level, *i.e.* 7.3 kcal/mol. They are in accord with the value of 16.8 kcal/mol obtained in a MRD CI calculation using a slightly

Table 3. Total energy of $^1A'$ ground state (in a.u.) and relative energy (in kcal/mol) of $^3A''$ state of monomeric HNO obtained at different calculational levels. Geometries optimized by RHF/6-31G* for singlet and ROHF/6-31G* for triplet

	SCF	MP2	MP3	MP4[a]	CISD[b]
E_{tot} (a.u.)	− 129.78607	− 130.11862	− 130.12264	− 130.14172	− 130.13364
E_{rel} (kcal/mol)	7.3	23.9	19.3	20.5	16.0

[a] MP4(SDTQ)
[b] Size-consistency corrected value

Table 4. Geometries (in Å and degrees), energies (in a.u.) and zero-point energies (ZPE) (in kcal/mol) for *cis*-dimer of HNO. Basis 6-31G*

	HF	MP2	QCISD
R(N–N)	1.2471	1.3646	1.3076
R(N–O)	1.2307	1.2477	1.2541
R(N–H)	1.0091	1.0319	1.0307
∠(O–N–N)	125.68	123.77	124.61
∠(H–N–N)	114.36	113.00	113.66
$\omega(O^1\text{–}N\text{–}N\text{–}H^2)$	180.00	180.65	180.01
E(a.u.)			
HF	− 259.55184		
MP2	− 260.27135	− 260.28423	
MP4(SDTQ)	− 260.30806	− 260.32197	
QCISD			− 260.27877
QCISD(T)			− 260.30925
ZPE (kcal/mol)	27.05		

different basis set [48]. A full CI calculation in the same paper led to a value of 15.7 kcal/mol.

The two different dimeric forms of **10**, *viz. cis* and *trans*, have the symmetries C_{2v} and C_{2h}, respectively. The completely optimized geometries of the two forms obtained at the SCF, MP2 and QCISD levels are found in Table 4 and Table 5. They show that both forms, species **11** and **12**, optimized to planar geometries having the symmetries mentioned above. The optimized geometries of **11** and **12**, using correlated wavefunctions, show some deviations from the corresponding ones obtained at the SCF level. The most significant change is the increase in the predicted N–N bond length, which is particularly large at the MP2 level. The energy difference between the two forms is not found to be significantly dependent on the level of calculation. Our best calculations, MP4(SDTQ)//MP2 and QCISD(T)//QCISD, give differences of 5.2 kcal/mol and 5.7 kcal/mol, respectively, in favour of the *trans* form. The latter difference is modified to 5.5 kcal/mol after correcting for differences in ZPE obtained at the QCISD level.

The association of two monomers in their ground state, ^{1}**A**′, to ground state of species **11** and **12** is symmetry forbidden under the symmetry constraints C_{2h} and C_{2v}, respectively. These least-motion approaches lead to avoided crossings, as the ground state monomers correlate with the exited states of the dimers under these

Table 5. Geometries (in Å and degrees), energies (in a.u.) and zero-point energies (ZPE) (in kcal/mol) for *trans*-dimer of HNO. Basis 6-31G*

	HF	MP2	QCISD
R(N–N)	1.2360	1.3578	1.2980
R(N–O)	1.2451	1.2535	1.2658
R(N–H)	1.0117	1.0339	1.0316
∠(O–N–N)	124.84	124.51	125.39
∠(H–N–N)	113.19	110.84	112.09
$\omega(O^1\text{–}N\text{–}N\text{–}O^2)$	180.00	180.00	180.00
E(a.u.)			
HF	− 259.56350		
MP2	− 260.27740	− 260.29030	
MP4(SDTQ)	− 260.31628	− 260.33029	
QCISD			− 260.28808
QCISD(T)			− 260.31825
ZPE (kcal/mol)	26.83	23.86	24.19

symmetry constraints. An orbital correlation diagram for the *trans* species is given in Fig. 2. This implies that the least motion path for this reaction has a substantial barrier E_a. For **11** we have relaxed all remaining geometry parameters under C_{2h} symmetry for fixed N...N distances at the RHF/6-31G* level. We found an energy maximum for an N...N distance of around 2.1 Å. This maximum lies about 150 kcal/mol above the ground state of **11**. The restricted wave function in this point was found to be unstable relative to an UHF solution. CISD calculations in this region revealed a contribution from the doubly exited configuration 16 → 17 to the total wavefunction. The value of its coefficient in the normalized wave function is around 0.15. The energy difference at this level of calculation was found to be 76.2 kcal/mol. These results demonstrate the forbiddenness of the least-motion approach.

In the search for a transition state for a non-least-motion dissociation of the dimeric *trans* form we were able to locate a stationary point on the potential surface, species **13**, having the predicted geometry displayed in Table 6. The search was made without any constraints on the internal coordinates which were fully relaxed during the optimization. The final structure has strictly a C_1 symmetry, but the differences between corresponding, nearly equivalent, geometry parameters are so small that within 0.0001 Å in bond distances and 0.002° in valence angles the symmetry is C_i. Furthermore, the calculated electric dipole moment is 0.00 Debye. The predicted structure of the transition state is found to be rather independent of the calculational level. The most significant difference found is an increase in the pyramidalization around the nitrogen atoms, the sum of the angles around these atoms being 325.2 and 336.8 degrees using HF and correlated wavefunctions, respectively. The planes through each of the NHO moieties are virtually parallel. The oxygen atoms are in quasi *trans* position relative to each other.

The stationary point corresponding to species **13** has one imaginary frequency of $615i\ cm^{-1}$ at the UHF level. The associated normal vibration is dominated by a nitrogen–nitrogen stretch. This implies that the transition state found is the correct one for the dissociation of the dimer in its *trans* form.

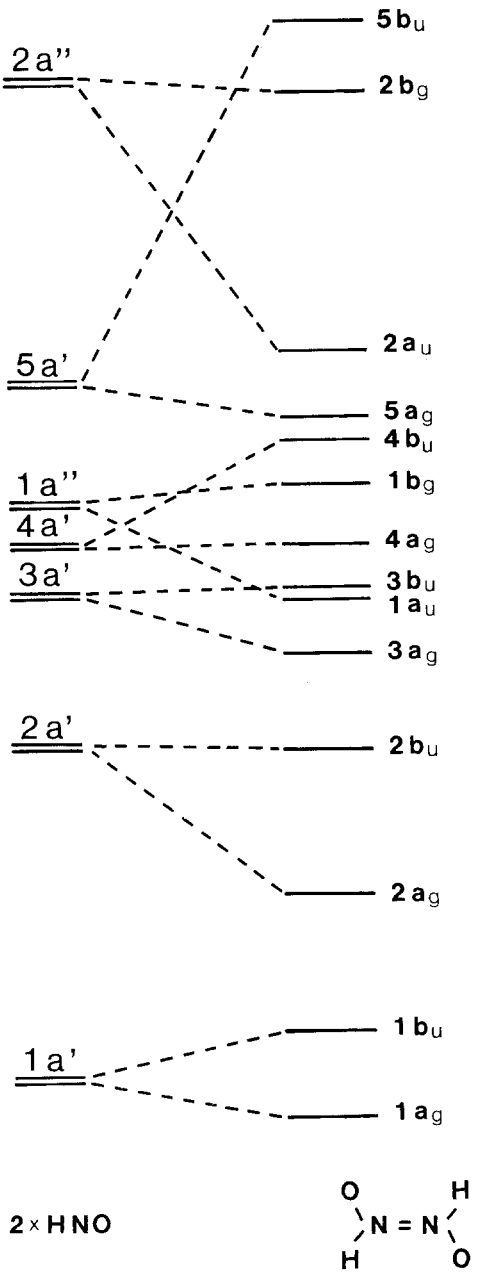

Fig. 2. Optimized correlation diagram for the reaction 2 HNO → $(HNO)_2$ in an approach under C_{2h} symmetry

The UHF solution for species **13** has a large spin contamination. The expectation value of S^2 was found to be 1.1468. After projecting out the lowest triplet this value increased to 1.5062. The calculated atomic spin densities are + 0.76 on O^1, − 0.40 on N^1, + 0.40 on N^2 and − 0.76 on O^2. See Fig. 1 for labelling of atoms. These values show that there are significant residual spins on the N and O atoms,

Table 6. Geometries (in Å and degrees), energies (in a.u.) and zero-point energies (ZPE) (in kcal/mol) for the transisition state for dimerization to *trans*-dimer of HNO. Basis 6-31G*

	HF	MP2	QCISD
R(N....N)	1.8514	1.9140	1.8726
R(N–O)	1.2302	1.1848	1.2310
R(N–H)	1.0160	1.0590	1.0498
∠(O–N–N)	112.11	121.34	117.78
∠(H–N–N)	101.33	100.34	100.97
∠(H–N–O)	111.85	115.05	118.13
$\omega(H^1\text{–}N\text{–}N\text{–}H^2)$	179.90	178.18	179.39
E(a.u.)			
UHF	− 259.56221		
PUHF	− 259.59594		
UMP2	− 260.18615	− 260.19662	
PUMP2	− 260.21920	− 260.22695	
UMP4(SDTQ)	− 260.24491	− 260.25029	
PUMP4	− 260.27661	− 260.27904	
QCISD			− 260.25121
QCISD(T)			− 260.27611
ZPE (kcal/mol)	22.14	21.65	

Table 7. Total energy (in a.u.) of two non-interacting HNO ground state units, and relative energies (in kcal/mol) for *trans*-dimer, **11**, *cis*-dimer, **12**, and TS for *trans* dimerization, **13**, at different calculational levels. Values in parentheses for **13** are corrected for spin contamination. Basis 6-31G*

	2 × E(HNO)	**11**	**12**	**13**
SCF//SCF	− 259.57214	5.4	12.7	6.2(− 14.9)
MP2	− 260.23726	− 25.2	− 21.4	32.1(11.3)
MP4(SDTQ)	− 260.28346	− 20.6	− 15.4	24.2(4.3)
ZPE	20.16	26.83	27.05	26.83
MP2//MP2	− 260.24919	− 25.8	− 22.0	33.0(14.0)
MP4(SDTQ)	− 260.29611	− 21.5	− 16.2	28.8(10.7)
ZPE	17.38	23.86	23.30	21.65
QCISD//QCISD	− 260.27157	− 10.4	− 4.5	12.8
QCISD(T)	− 260.29353	− 15.5	− 9.9	10.9
ZPE	17.52	24.19	24.07	

and that the relative orientation of the spins permit couplings to an N... N bond or to N... O bonds depending on the direction of the reaction. The high value of the S^2 expectation value after annihilation of the lowest triplet implies significant contributions to the UHF wave function from higher spin states. Although geometries predicted by the UHF approximation usually are rather accurate, it has been shown to be crucial to remove spin contaminations from the SCF and UMPn wavefunctions in order to obtain reliable estimates of energies for species having one or more broken bonds. Different schemes for projecting out spin contaminations have been published [53–57]. In our case we have adopted the annihilation scheme implemented in Guassian 90 [42]. The results, given in Table 7, show that

the energy corrections due to proper treatment of spin contamination are substantial. In this case it is of particular interest to observe that spin states beyond $s + 1$ have a dramatic influence on the predicted relative energy of the transition state **13**. The projections applied are through $s + 4$ at all levels of calculation. Projections up to s + 6 at the UHF level did not change the results given in Table 7. Our estimates of the activation energy, E_a, for the association reaction (3) to the *trans* dimer are found to be rather dependent on the calculational level. It is, however, gratifying that approaches using correlated wavefunctions also in the geometry optimizations give about the same values after proper treatment of spin contamination. Thus the MP4(SDTQ)//MP2 value of 10.7 kcal/mol is in very good agreement with the QCISD(T)//QCISD value of 10.9 kcal/mol. Unscaled ZPE corrections, calculated at the SCF level, change these values to 12.7 and 12.9 kcal/mol, respectively.

In order to obtain a best possible estimate of the reaction energy ΔH for the association reaction:

$$2\ \mathrm{HNO}\ (^1A') \overset{K_p}{\rightleftarrows} \textit{trans}\text{-}(\mathrm{HNO})_2 \tag{3}$$

we have applied the G1 theory developed by Pople et al. [41]. Using this theory we predict an exothermic heat of reaction for the association equal to 16.4 kcal/mol. This value is rather good agreement with the energy difference of 15.0 kcal/mol obtained by the MP4//MP2 method with correction for unscaled ZPE. The QCISD(T)//QCISD approximation corrected for differences in ZPE gives a somewhat smaller value, *i.e.* 8.8 kcal/mol. A comparison of the total energies shown in Tables 1, 4 and 5 indicates that the QCI approximation leads to values that are a little too high for the dimeric forms. To our knowledge there are no experimental data available for this reaction of HNO. However, for the dissociation of *trans*-bisnitrosomethane into two CH_3NO units in the gas phase there are two experimental values available, *viz.* 18 ± 2 kcal/mol [59] and 16.6 ± 0.5 kcal/mol [31]. These values are very close to our predicted MP4 result for the HNO system.

Experimental dimerization energies for several C-nitroso compounds in solution are also available. Values reported [20] for α-nitroso-methyl isopropyl ketone, ω-nitroso-toluene and nitroso-cyclohexane are 18.9, 20.4 and 20.6 kcal/mol, respectively. Although caution should be observed in comparing our predicted values to these, because of heavy substituents and solvent effects, it is interesting to note that they are all rather close to our theoretical estimate for the HNO system.

Entropies for the monomer and *trans* dimer obtained by the 6-31G* basis are 0.053 and 0.062 kcal/mol/K, respectively. This leads to a ΔS value for the association reaction of -0.044 kcal/mol·K. Combining this with the approximate ΔH value obtained above, assuming the ΔH value to be temperature independent, we find a ΔG-value at 298 K of 3.29 kcal/mol. This corresponds to a calculated equilibrium constant (K_p) for the reaction (3) of 259 atm.

At the highest levels of calculation we predict a barrier of around 11 kcal/mol for the dimerization along a non-least-motion path. A ZPE correction estimated at the MP2 level changes this value to 15 kcal/mol. This rather low barrier combined with the large predicted value of K_p suggests that the *trans* dimer should be thermodynamically stable relative to the monomer at room temperature. We have, however, not considered alternative reaction channels for the dimer that might prevent its isolation.

Epilogue. We are pleased to dedicate this article to Professor Inga Fischer–Hjalmars considering her substantial contributions to molecular science. One of us (P.N.S.) will also express his thanks to her for inspiring teaching and supervision during his stay in Stockholm 1961–65.

Acknowledgement. The authors want to thank the Norwegian Research Council for Science and Humanities for granting CPU time on CRAY at the SINTEF Supercomputer Center. They are grateful to Prof. B. G. Gowenlock for his comments on the manuscript.

References

1. Baly C, Desch N (1908) J Chem Soc 93:1747
2. Piloty O (1898) Ber Dt Chem Ges 31:456,1878; (1901) ibid 34:1863; (1902) ibid 35:3090,3101
3. Darwin C, Hodgkin DC (1950) Nature 166:827
4. Fenimore CP (1950) J Am Chem Soc 72:3226
5. Lüttke W (1954) J Physique et la Radium 15:633
6. Lüttke W (1955) Angew Chem 67:235; (1956) ibid 68:417; (1957) ibid 69:99
7. Lüttke W (1956) Habilitationsschrift Univ Freiburg i. Br.
8. Lüttke W (1957) Z f Elektrochemie 61:302,976
9. Kübler R, Lüttke W, Weckherlin S (1960) Z f Elektrochemie 64:657
10. Hammick DL (1931) J Chem Soc 3105
11. Chilton HTJ, Gowenlock BG, Trotman J (1955) Chem and Ind 538
12. Gowenlock BG, Trotman J (1955) J Chem Soc 4190; (1956) ibid 1670
13. van Meersche M, Germain G (1959) Bull Soc Chim Belges 68:24411
14. Germain G, Piret P, van Meersche M (1963) Acta Cryst 16:109
15. Leroy G, van Meersche, M, Germain G (1963) J Chim. Physique 1282; Leroy G, Martin P, Peeters D (1974) ibid 319
16. Orgel LE (1953) J Chem Soc 1276
17. Wu AA, Peyerimhoff SD, Buenker RJ (1975) Chem Phys Lett 35:316
18. Herzberg G (1966) Molecular spectra and molecular structure III: Electronic spectra and electronic structure of polyatomic molecules. Van Nostrand Reinhold, p 289, 496, 598
19. Gowenlock BG, Lüttke W (1958) Quart Rev Chem Soc 12:321
20. von Keussler V, Lüttke W (1959) Z f Elektrochemie 63:614
21. Tarte P (1954) Bull Soc Chim Belges 63:525
22. Mc Ewen KL (1961) J Chem Phys 34:547
23. Ha TK, Wild UP (1974) Chem Phys 4:300
24. Bhujle V, Wild UP, Baumann H, Wagnière G (1976) Tetrahedron 9:653
25. Boyer JH (1969) in: Feuer H (ed) The chemistry of the nitro and nitroso groups. Interscience, NY, Part 1, Chap 5, p 264
26. DMS UV atlas of organic compounds. Verlag Chemie, Weinheim, 1971, Spectrum no. C4/1
27. Hoffmann R, Gleiter R, Mallory FB (1970) J Am Chem Soc 92:1461
28. Minato T, Yamabe S, Oda H (1982) Can J Chem 60:2740
29. Yamabe S, Minato T, Osamura Y (1980) Int J Quant Chem 18:243
30. Heiberg AB (1977) Chem Phys 26:309; ibid 43:415
31. Christie MI, Frost JS, Voisey MA (1965) Trans Faraday Soc 61:674
32. Hughes MN (1968) Quart Rev Chem Soc 22:1
33. Kohout FC, Lampe FW (1967) J Chem Phys 46:4075
34. (a) He Y, Sanders WA, Lin MC (1988) J Phys Chem 92:5474; (b) Choudhury TK, He Y, Sanders WA, Lin MC (1990) ibid 94:2394
35. Tsang W, Herron JT (1991) J Phys Ref Data 20:646
36. Coe CS, Doumani TF (1948) J Am Chem Soc 70:1516
37. Tarte P (1953) Bull Soc Roy Liège 22:26
38. Hehre WJ, Ditchfield R, Pople JA (1972) J Chem Phys 56:2257
39. Hariharan PC, Pople JA (1975) Theor Chim Acta 28:213
40. Pople JA, Head–Gordon M, Raghavachari K (1987) J Chem Phys 87:5968
41. Pople JA, Head–Gordon M, Fox DJ (1989) J Chem Phys 90:5622

42. GAUSSIAN 90 Frisch MJ, Head–Gordon M, Trucks GW, Foresman JB, Schlegel HB, Raghavachari K, Robb MA, Binkley JS, Gonzales C, Defrees DJ, Fox DJ, Whiteside RA, Seeger R, Melius CF, Baker J, Martin RL, Kahn LR, Stewart JJP, Topiol S, Pople JA (1991) Carnegie-Mellon Quantum Chemistry Publ Unit, Pittsburgh PA
43. Callear AB, Wood PM (1971) Trans Faraday Soc 67:3399
44. Krauss M (1969) J Res Natl Bur Std US 73A:191
45. Salotto AW, Burnelle L (1969) Chem Phys Lett 3:80
46. Williams GR (1975) Chem Phys Lett 30:495
47. Wu AA (1977) Chem Phys 21:173
48. Bruna PJ, Marian CM (1979) Chem Phys Lett 67:109
49. Heiberg A, Almløf J (1982) J Chem Phys Lett 85:542
50. Walch SP, Rohlfing CM (1989) J Chem Phys 91:2939
51. Dalby FW (1958) Can J Phys 36:1366
52. Petersen JC (1985) J Mol Spectrosc 110:277
53. Gill PMW, Radom L (1986) Chem Phys Lett 132:16
54. Sosa C, Schlegel HB (1986) Int J Quant Chem 29:1001
55. Schlegel HB (1986) J Chem Phys 84:4530
56. Knowles PJ, Handy NC (1988) J Chem Phys 88:6691
57. Yamaguchi K, Takahara Y, Fueno T, Houk KN (1988) Theor Chim Acta 73:337
58. Stark JG, Wallace HG (1988) Chem data book. John Murray, London
59. Batt L, Milne RT (1973) Int J Chem Kinet 5:1067